

${}^6\text{He}+p$ 反応を通した 共鳴状態の解析

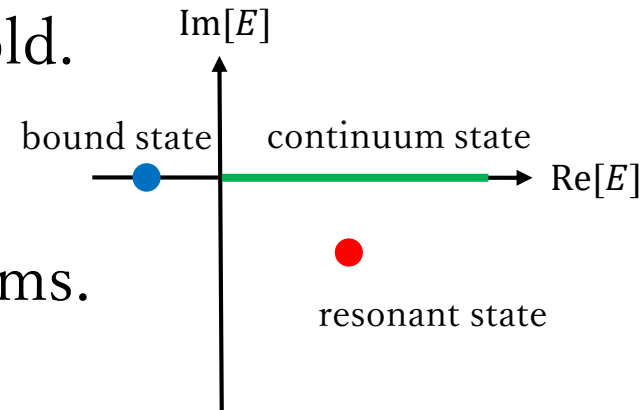
小川翔也 松本琢磨
九州大学

2019/12/23

“理研-九大ジョイントワークショップ「数理が紡ぐ素粒子・原子核・宇宙」” @ 九大

Resonant state

- ✓ Resonant states locate above the threshold.
- ✓ The pole of S matrix

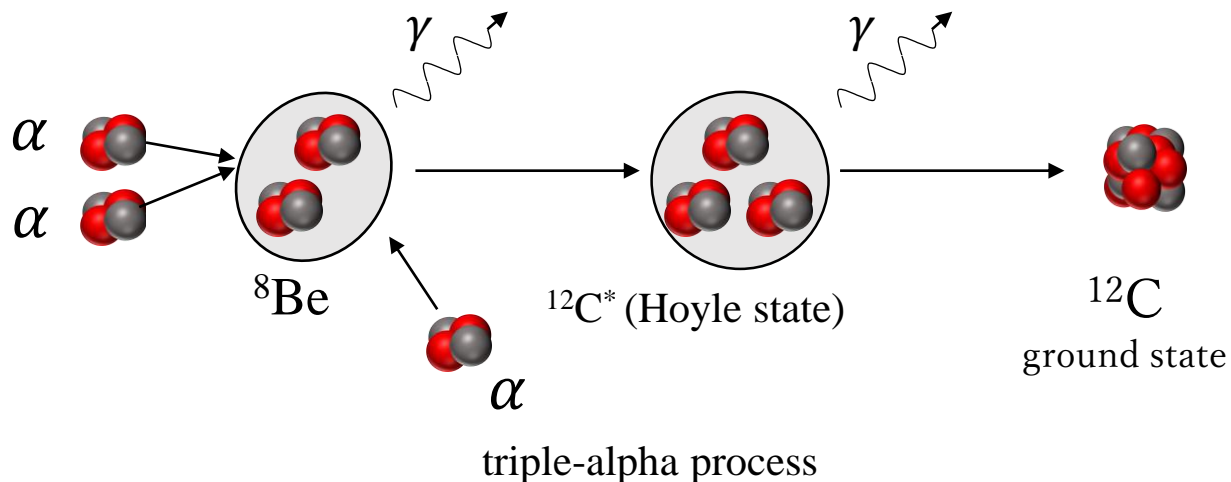


Resonant states appear in many-body systems.

ex) nucleons, quarks, atomics ...

Relationship with nucleosynthesis

ex) The resonant states of ^{12}C , 0_2^+ (Hoyle state)



Nuclear physics

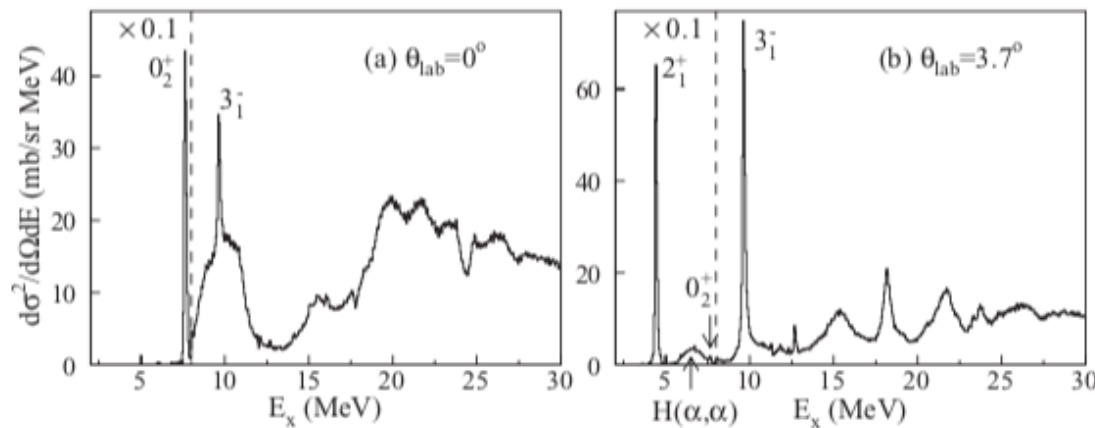
ex) Resonant states of ^{12}C

Reaction

- (p, p') or (α, α') reactions
- Energy spectrum

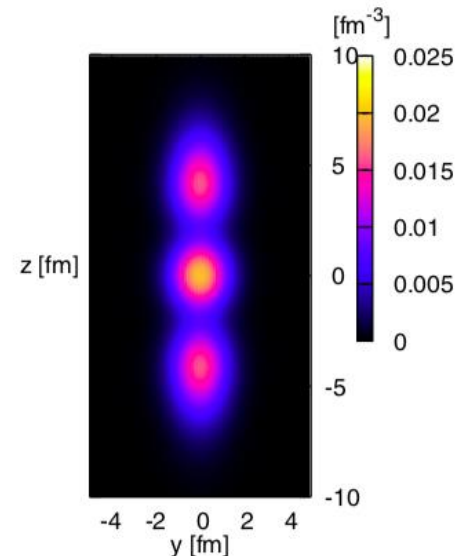
α - ^{12}C 散乱 @ $E_\alpha = 386$ MeV

M. Itoh *et al.*, Phys. Rev. C **84**, 054308 (2011).



Structure

- The 0_4^+ is considered as a nucleus having the linear-chain configuration of 3α .



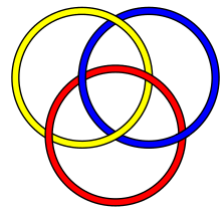
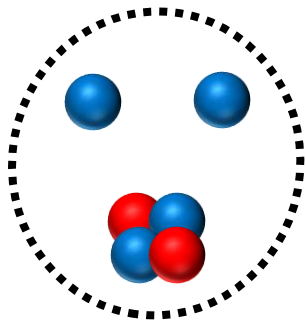
Y. Funaki,
Phys. Rev. C **94**, 024344 (2016)

Unstable nuclei

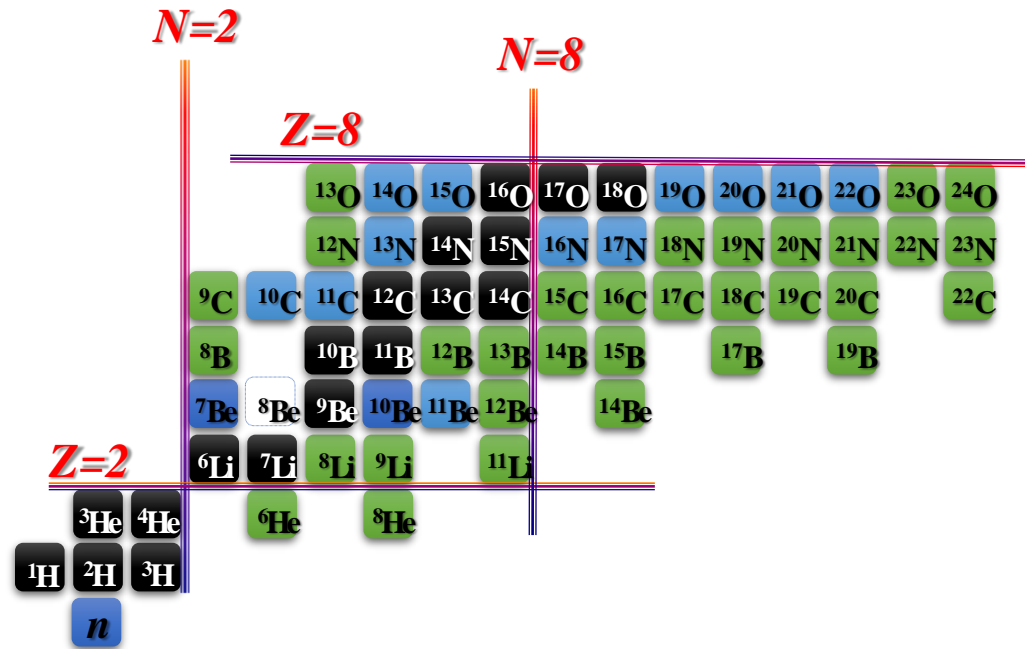
Recently, resonant states of nuclei near neutron dripline have been investigated intensively.

${}^6\text{He}$

- two neutron halo nuclei
- Borromean nuclei



(from Wikipedia)
Borromean rings



The resonant states of ${}^6\text{He}$ is analyzed via (p, p') reactions with inverse kinematics.

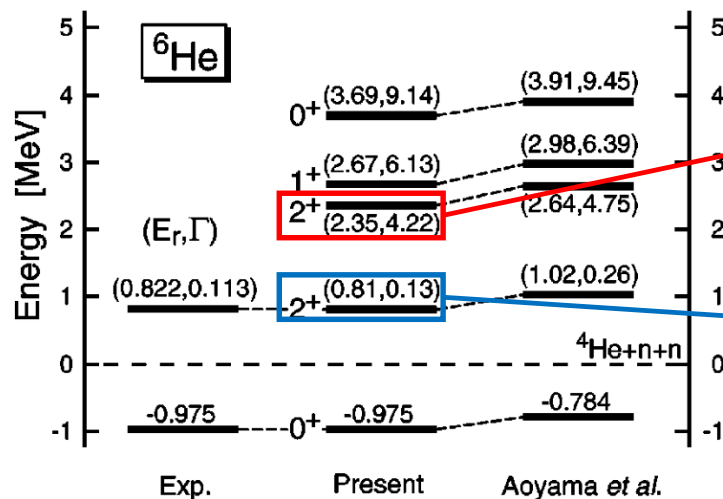
A. Lagoyannis *et al.*, Phys. Lett. B **518** (2001), 27.

B. S. V. Stepanov, *et al.*, Phys. Lett. B **542** (2002), 35.

Previous study on ${}^6\text{He}$

- ✓ The experimental data of (p, p') are analyzed by a calculation without coupling effects of between various states.
- ✓ The 2_2^+ state have been discussed by structural calculation.
 - This states is considered as the next lower state to the 2_1^+ .

T. Myo, *et al.*, Phys. Rev. C **63** (2001), 054313



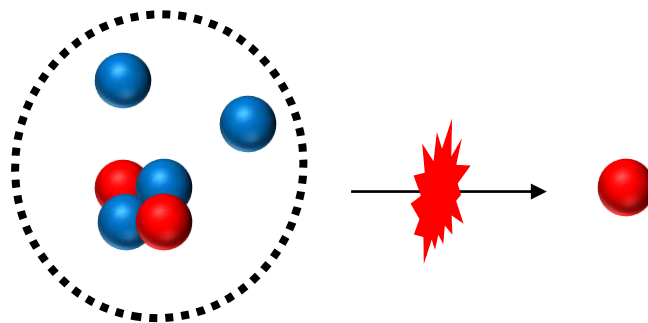
The 2_1^+ appears as a sharp peak in energy spectrum.
→ well understood.

It is not clear that how the 2_2^+ effects on cross sections.

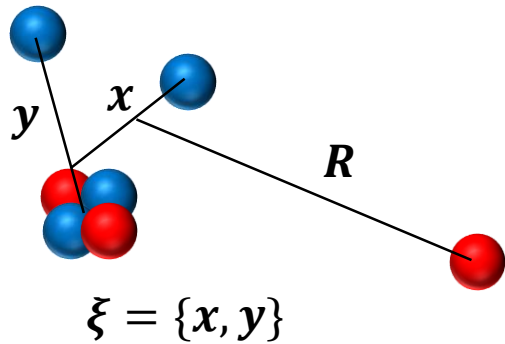
Purpose and Strategy

We analyze the effects from 2_2^+ on the observables via ${}^6\text{He}(p, p')$ reactions.

- Resonant state
 - ✓ ${}^6\text{He}$ is described as $\alpha+n+n$ system.
 - ✓ Complex Scaling Method (CSM)
- Analysis of ${}^6\text{He}(p, p')$ reactions
 - ✓ The ${}^6\text{He}+p$ reaction is the $\alpha+n+n+p$ four-body reaction.
 - ✓ Continuum-Discretized Coupled Channels method



Continuum-Discretized Coupled Channels method (CDCC)



Schrödinger equation

$$\left[K_R + \sum_i v_i + V_C + h^6\text{He} - E \right] \Psi(\xi, R) = 0$$

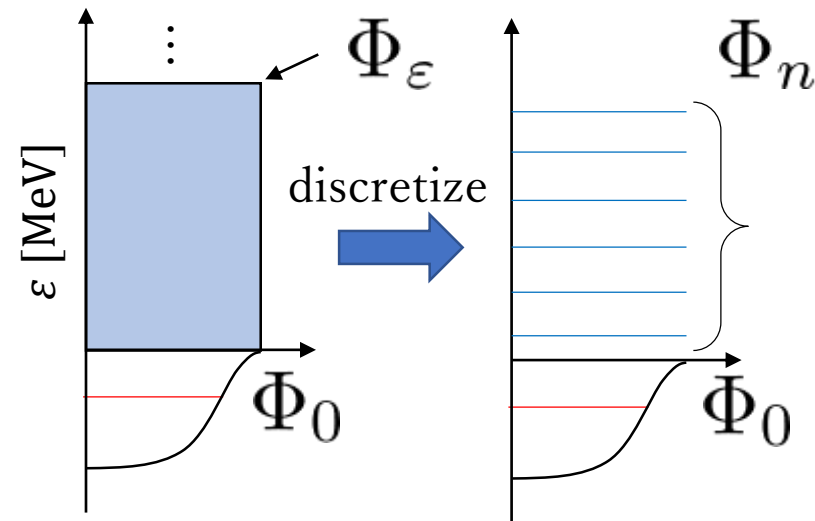
Continuum states of ${}^6\text{He}$ Φ_ϵ are discretized.

$$\Psi(\xi, R) = \Phi_0(\xi)\psi_0(R) + \int d\epsilon \Phi_\epsilon(\xi)\psi_\epsilon(R)$$

↓

$$\Psi(\xi, R) \approx \boxed{\Phi_0(\xi)}\psi_0(R) + \sum_i^{i_{\max}} \boxed{\Phi_n(\xi)}\psi_n(R)$$

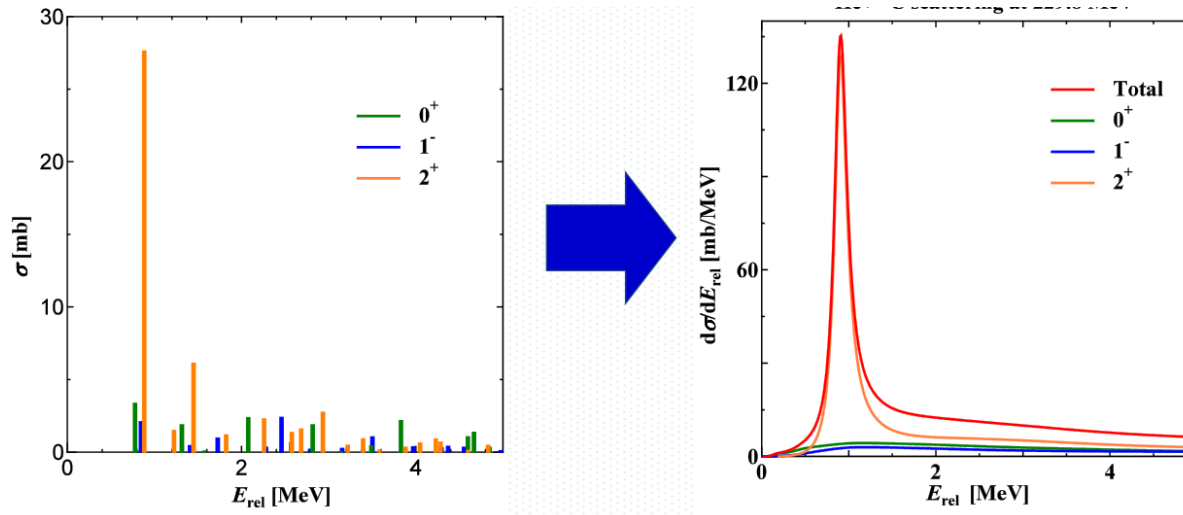
bound discretized-continuum



In the CDCC, we solve the coupled-channels equation considering the couplings between the discretized states.

Smoothing factor

Obtained cross sections are discretized in eigen energies.



- CDCC + CSM T. Matsumoto, *et al.*, Phys. Rev. C **82** (2010), 051602(R)

$$\frac{d^2\sigma}{d\epsilon d\Omega} = \frac{1}{\pi} \sum_{\nu} \sum_{i,j} T_i^{\text{CDCC}\dagger} \underbrace{\frac{\langle \Phi_i | U(-\theta) | \Phi_{\nu}^{\theta} \rangle \langle \tilde{\Phi}_{\nu}^{\theta} | U(\theta) | \Phi_j \rangle}{\epsilon - \epsilon_{\nu}^{\theta}}}_{\text{obtained by CSM}} T_j^{\text{CDCC}}$$

T_i^{CDCC} : T matrix calculated with CDCC

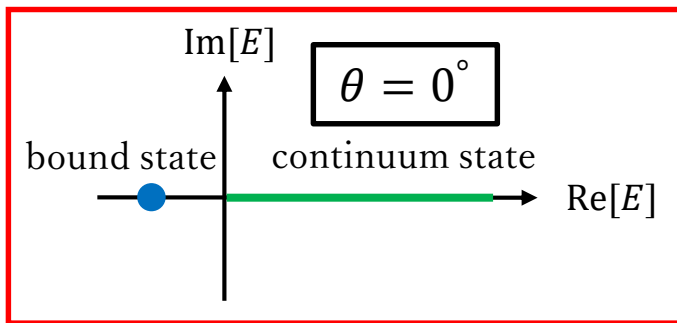
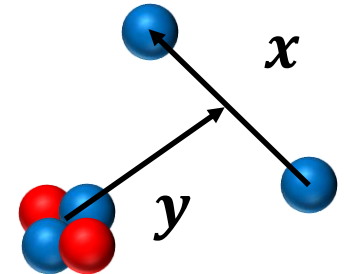
We can **separate the part of resonant states** from $d^2\sigma/d\epsilon d\Omega$.

➡ We can evaluate the contribution from resonant states to the cross section.

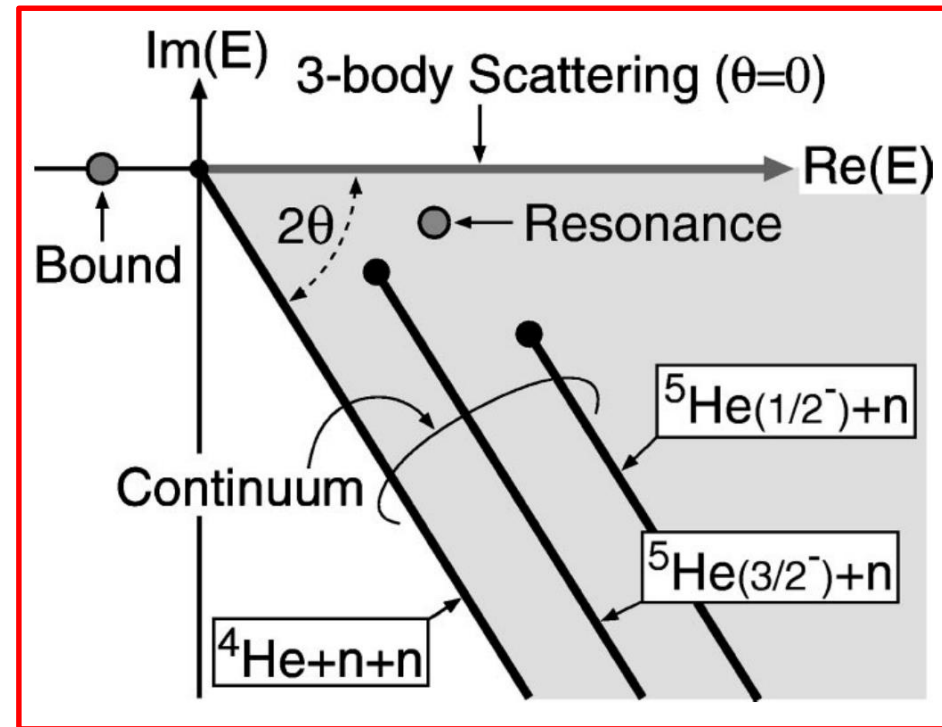
Complex Scaling Method (CSM)

We consider the transformation as followings.

$$U(\theta)\mathbf{x}U^{-1}(\theta) = \mathbf{x}e^{i\theta}, \quad U(\theta)\mathbf{y}U^{-1}(\theta) = \mathbf{y}e^{i\theta}$$



$$\theta \neq 0^\circ$$



Resonant states appear as isolated poles.

$$E_{\text{res}} = E_r - i\frac{\Gamma}{2}$$

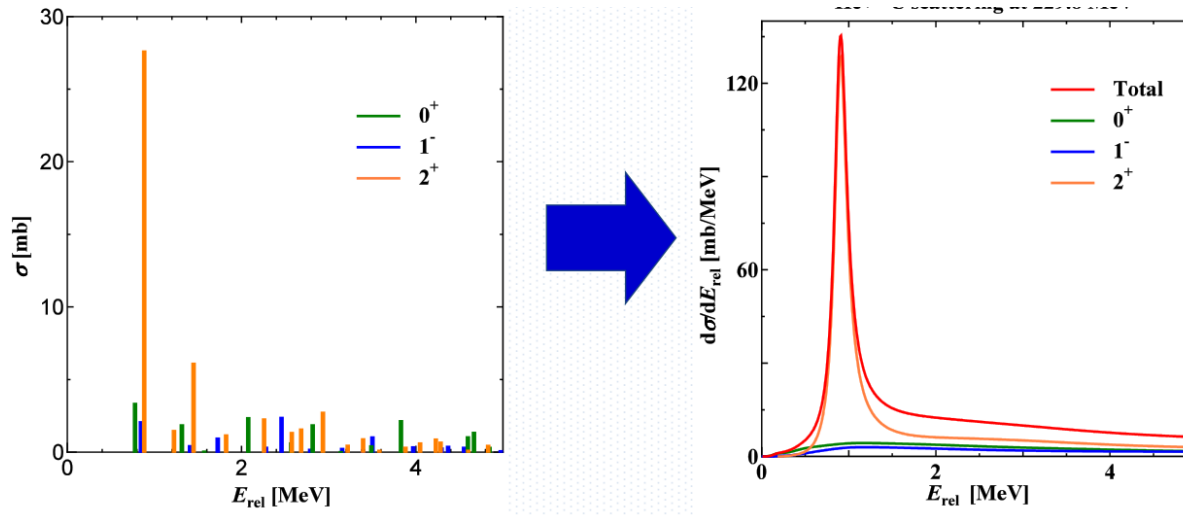
resonance energy

decay width

T. Myo, *et al.*, Phys Rev C 63 (2001), 054313

Smoothing factor

Obtained cross sections are discretized in eigen energies.



- CDCC + CSM T. Matsumoto, *et al.*, Phys. Rev. C **82** (2010), 051602(R)

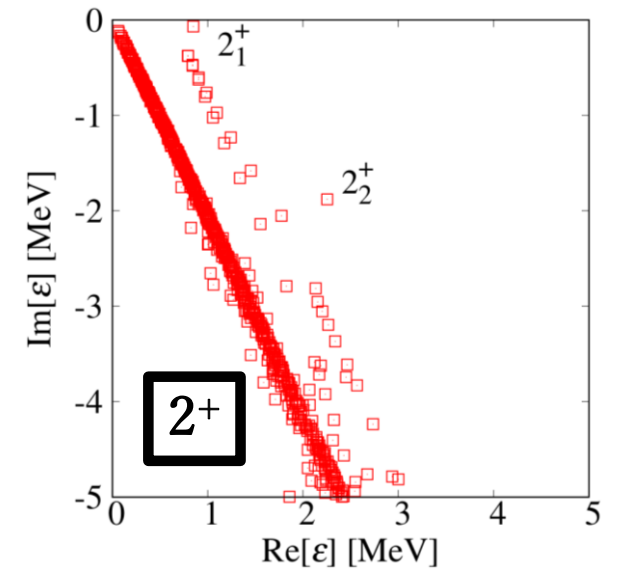
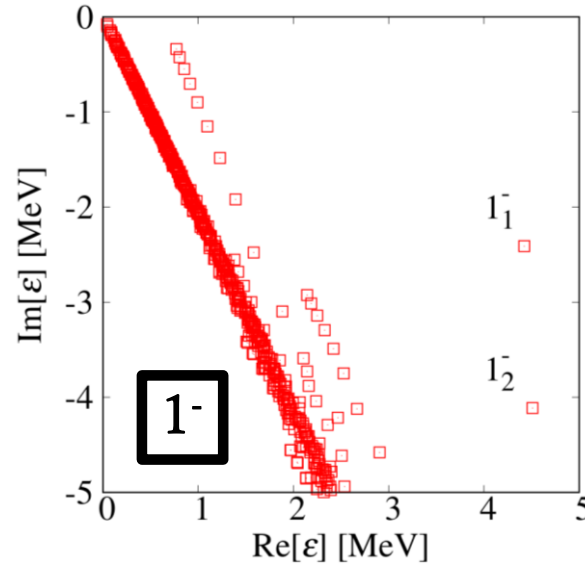
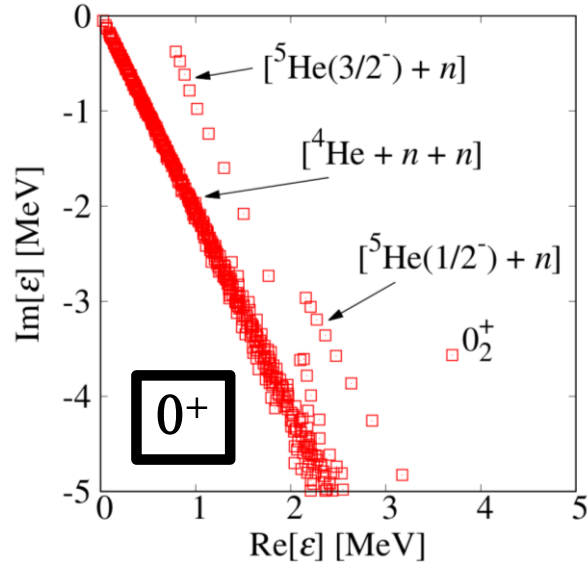
$$\frac{d^2\sigma}{d\varepsilon d\Omega} = \frac{1}{\pi} \sum_{\nu} \sum_{i,j} T_i^{\text{CDCC}\dagger} \underbrace{\frac{\langle \Phi_i | U(-\theta) | \Phi_{\nu}^{\theta} \rangle \langle \tilde{\Phi}_{\nu}^{\theta} | U(\theta) | \Phi_j \rangle}{\varepsilon - \varepsilon_{\nu}^{\theta}}}_{\text{obtained by CSM}} T_j^{\text{CDCC}}$$

T_i^{CDCC} : T matrix calculated with CDCC

We can **separate the part of resonant states** from $d^2\sigma/d\varepsilon d\Omega$.

➡ We can evaluate the contribution from resonant states to the cross section.

Results of CSM

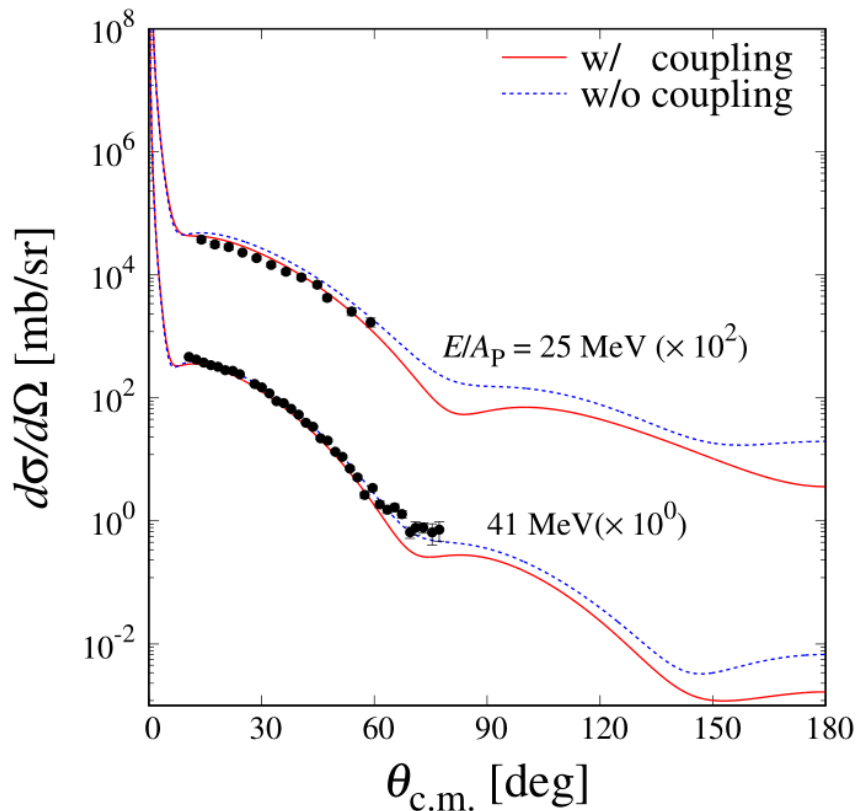


	Calc.		T. Myo, <i>et al.</i> [1]	
J^π	E_r	Γ	E_r	Γ
2_1^+	0.85	0.14	0.81	0.13
2_2^+	2.25	3.75	2.35	4.22
0_2^+	3.70	7.13	3.69	9.14
1_1^-	4.42	4.82		
1_2^-	4.51	8.23		

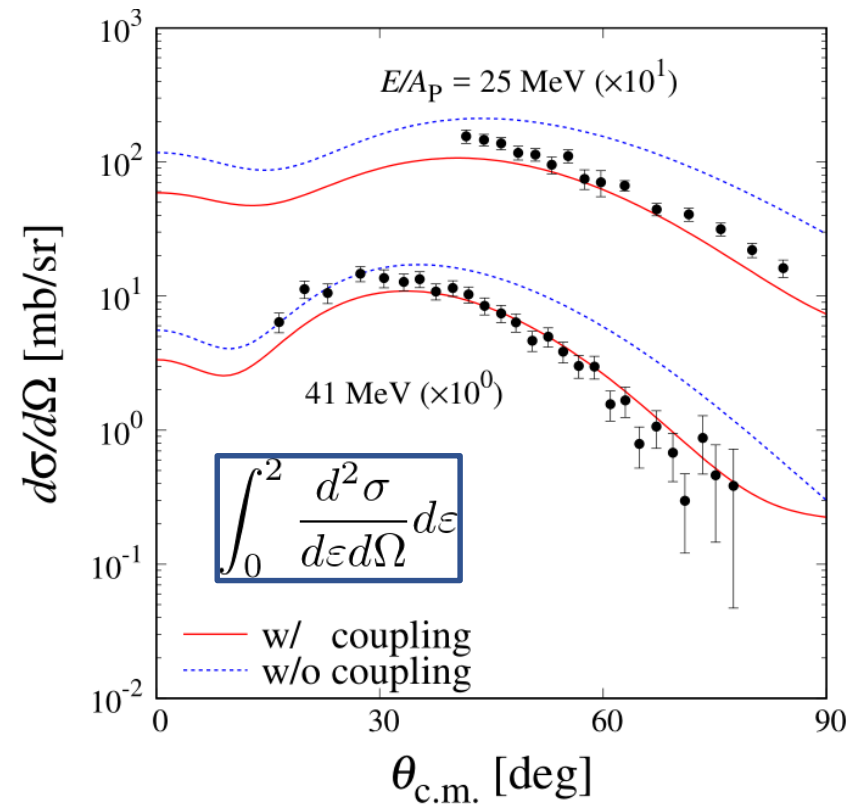
[1] T. Myo, *et al.*, Phys. Rev. C **63** (2001), 054313

Elastic and Inelastic cross sections

elastic

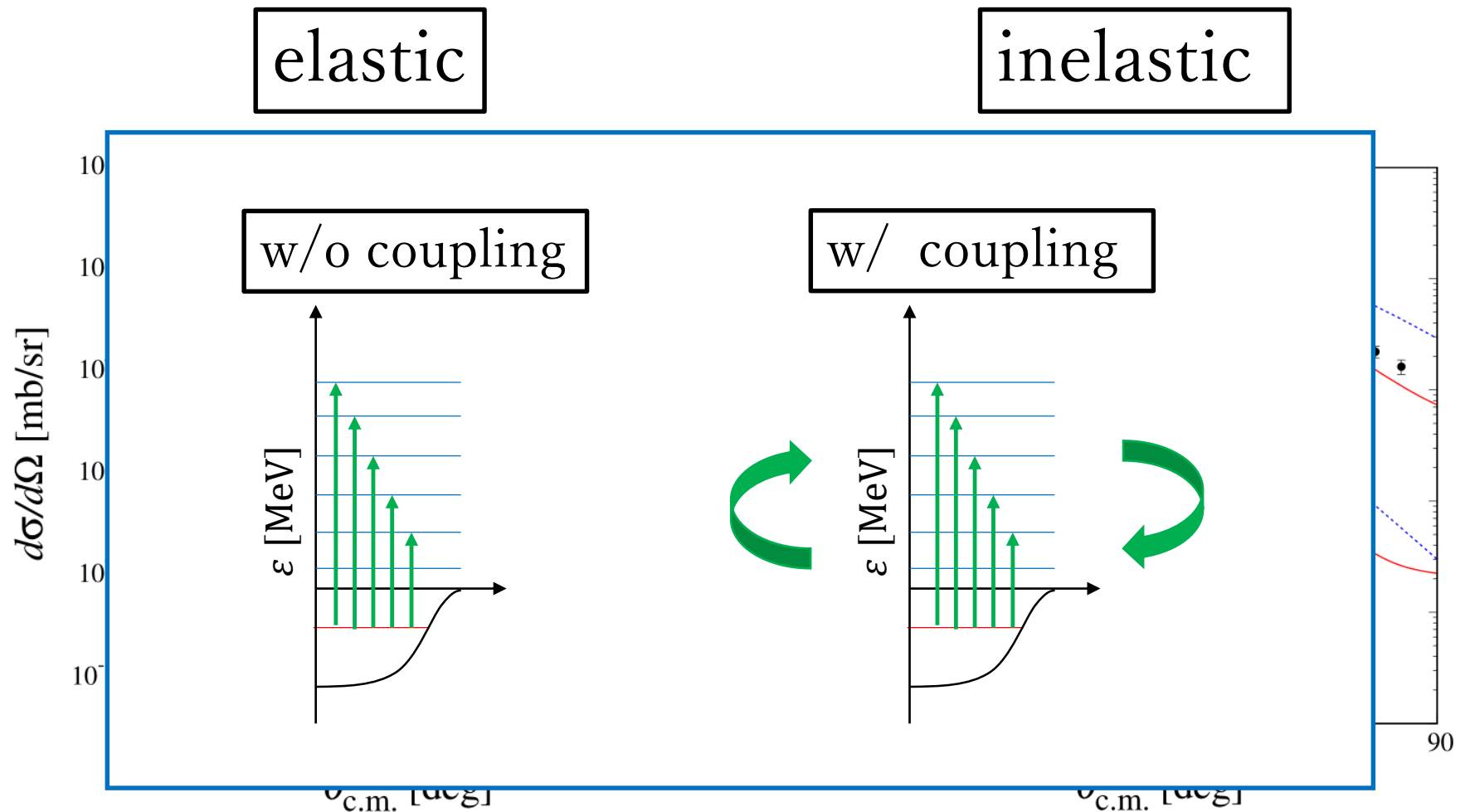


inelastic



- ✓ The results of CDCC reproduce well the experimental data.
- ✓ Coupling effects are important.

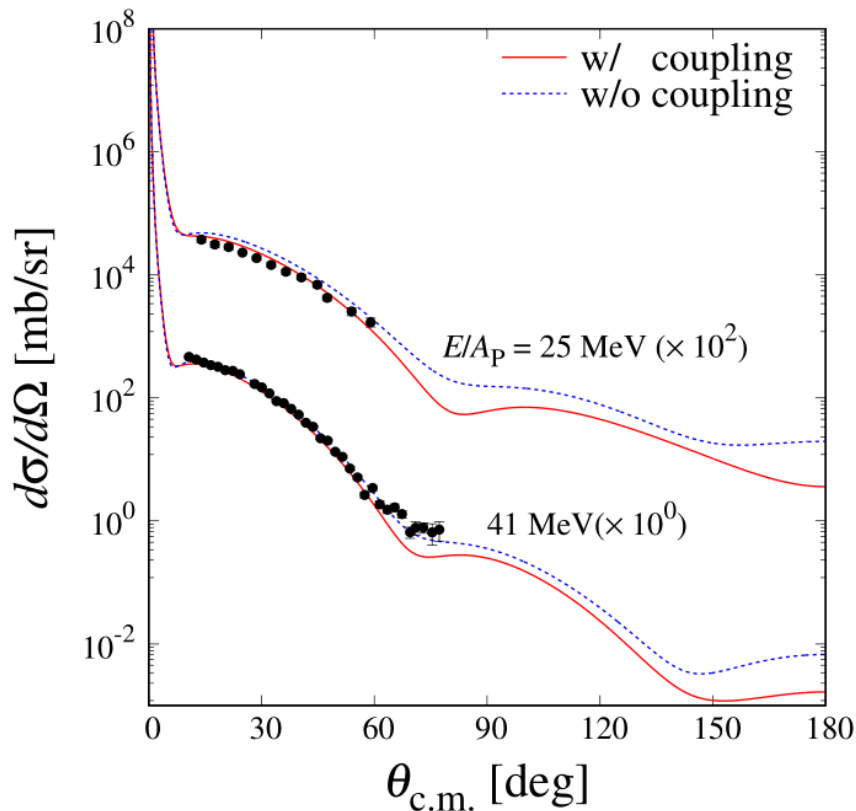
Elastic and Inelastic cross sections



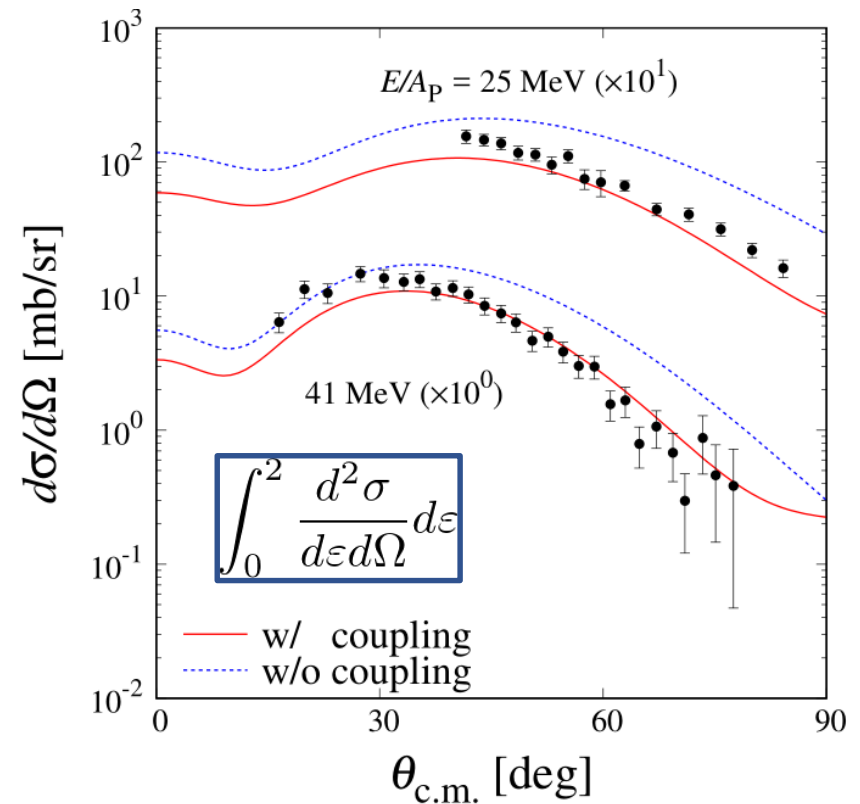
- ✓ The results of CDCC reproduce well the experimental data.
- ✓ Coupling effects are important.

Elastic and Inelastic cross sections

elastic



inelastic



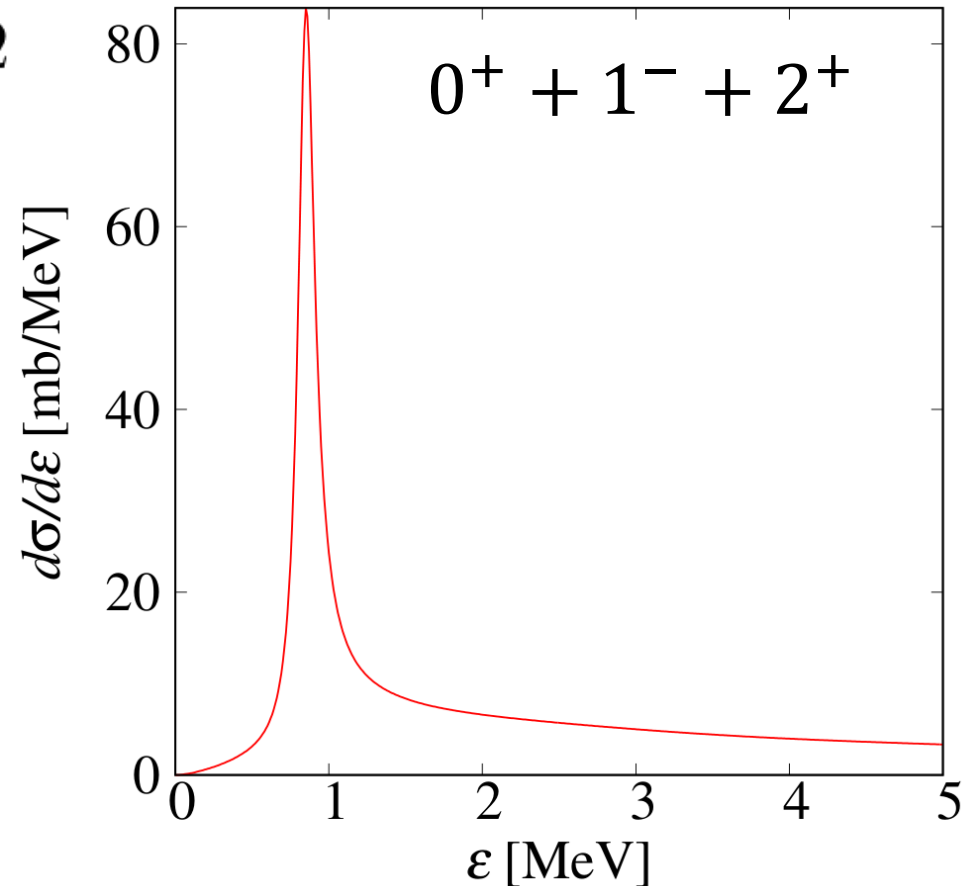
- ✓ The results of CDCC reproduce well the experimental data.
- ✓ Coupling effects are important.

Energy spectrum

$$E/A=41\text{MeV}$$

$$\frac{d\sigma}{d\varepsilon} = \int_{0^\circ \leq \theta \leq 180^\circ} \frac{d^2\sigma}{d\varepsilon d\Omega} d\Omega$$

Calc.		
I^π	E	Γ
2_1^+	0.848	0.136
2_2^+	2.25	3.75
0_2^+	3.70	7.13
1_2^-	4.51	8.23
1_1^-	4.42	4.82



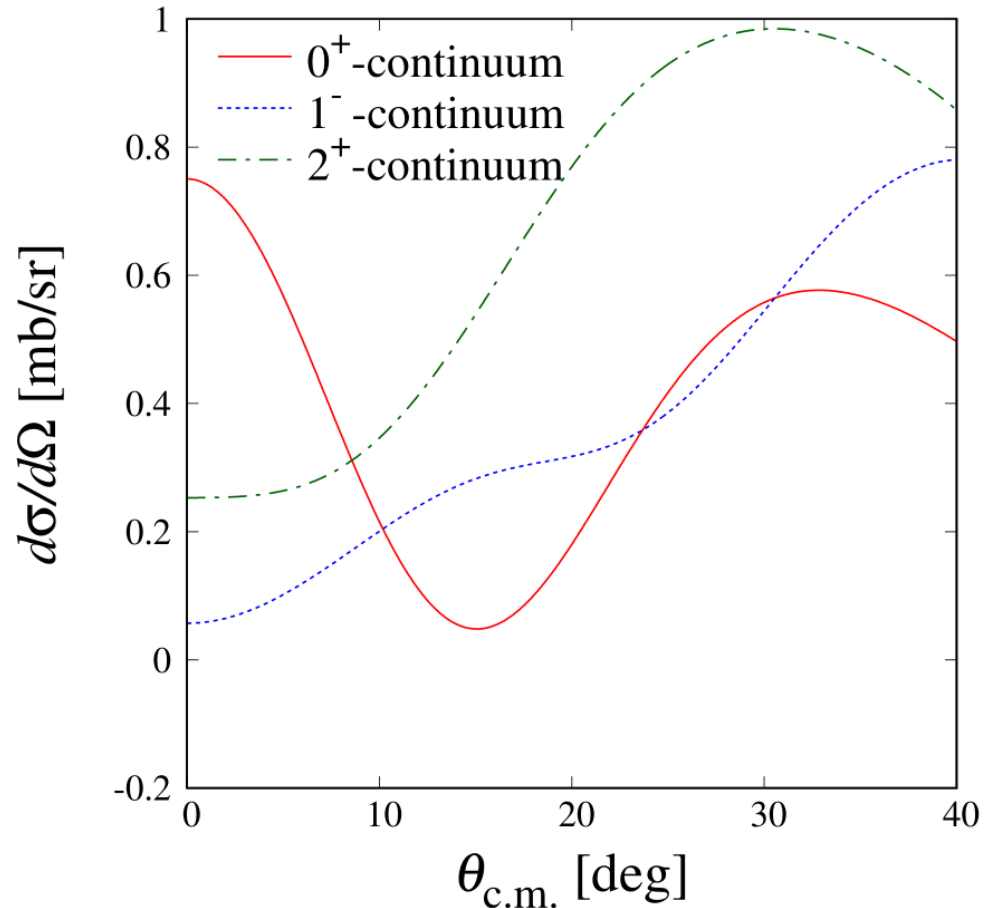
- The 2_1^+ appear as the sharp peak.
- A clear peak from 2_2^+ can not be seen.

Angular distribution

$$E/A=41\text{MeV}$$

$$\frac{d\sigma}{d\Omega} = \int_{\underline{2} \leq \varepsilon \leq \underline{3}} \frac{d^2\sigma}{d\varepsilon d\Omega} d\varepsilon$$

Calc.		
I^π	E	Γ
2_1^+	0.848	0.136
2_2^+	2.25	3.75
0_2^+	3.70	7.13
1_2^-	4.51	8.23
1_1^-	4.42	4.82



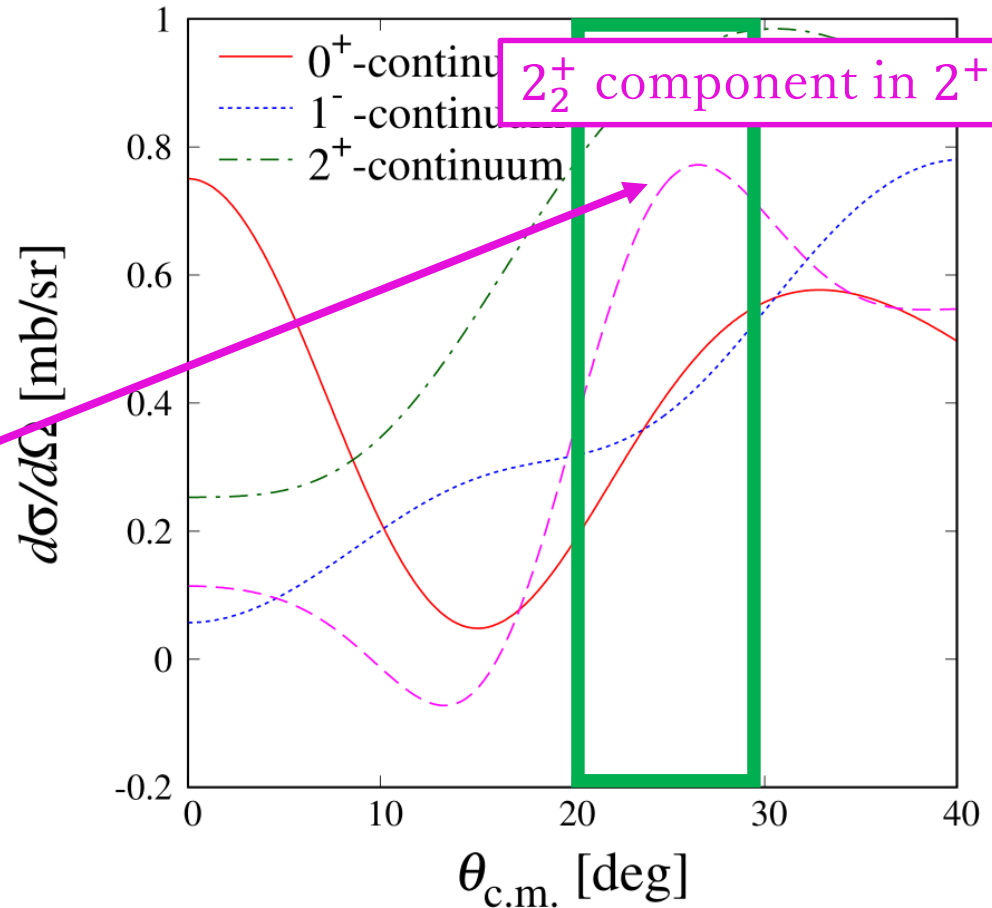
- 2^+ -continuum : relatively large in $20^\circ \sim 30^\circ$

Angular distribution

$$E/A=41\text{MeV}$$

$$\frac{d\sigma}{d\Omega} = \int_{2 \leq \varepsilon \leq 3} \frac{d^2\sigma}{d\varepsilon d\Omega} d\varepsilon$$

Calc.		
I^π	E	Γ
2_1^+	0.848	0.136
2_2^+	2.25	3.75
0_2^+	3.70	7.13
1_2^-	4.51	8.23
1_1^-	4.42	4.82



- The effect of 2_2^+ is enhanced in $20^\circ \sim 30^\circ$.

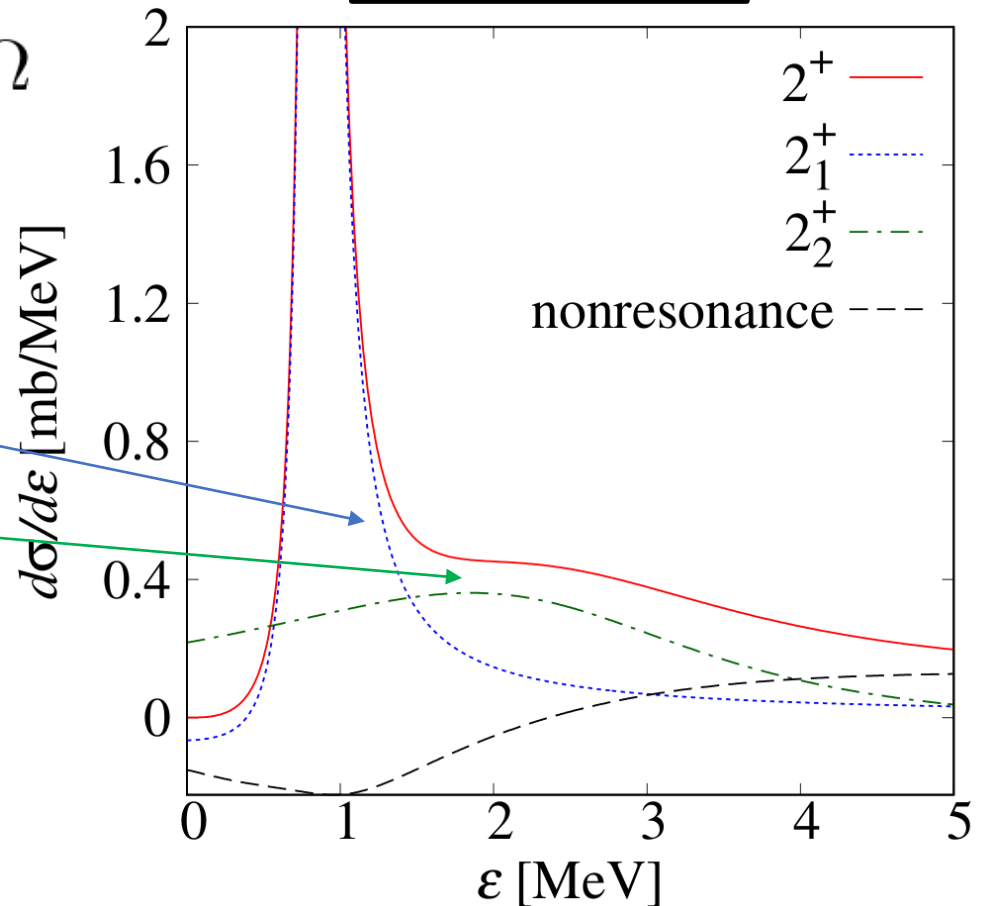
Energy spectrum (2^+)

$$E/A=41\text{MeV}$$

$$\frac{d\sigma}{d\varepsilon} = \int_{20^\circ \leq \theta \leq 30^\circ} \frac{d^2\sigma}{d\varepsilon d\Omega} d\Omega$$

Calc.		
I^π	E	Γ
2_1^+	0.848	0.136
2_2^+	2.25	3.75
0_2^+	3.70	7.13
1_2^-	4.51	8.23
1_1^-	4.42	4.82

2^+ -continuum



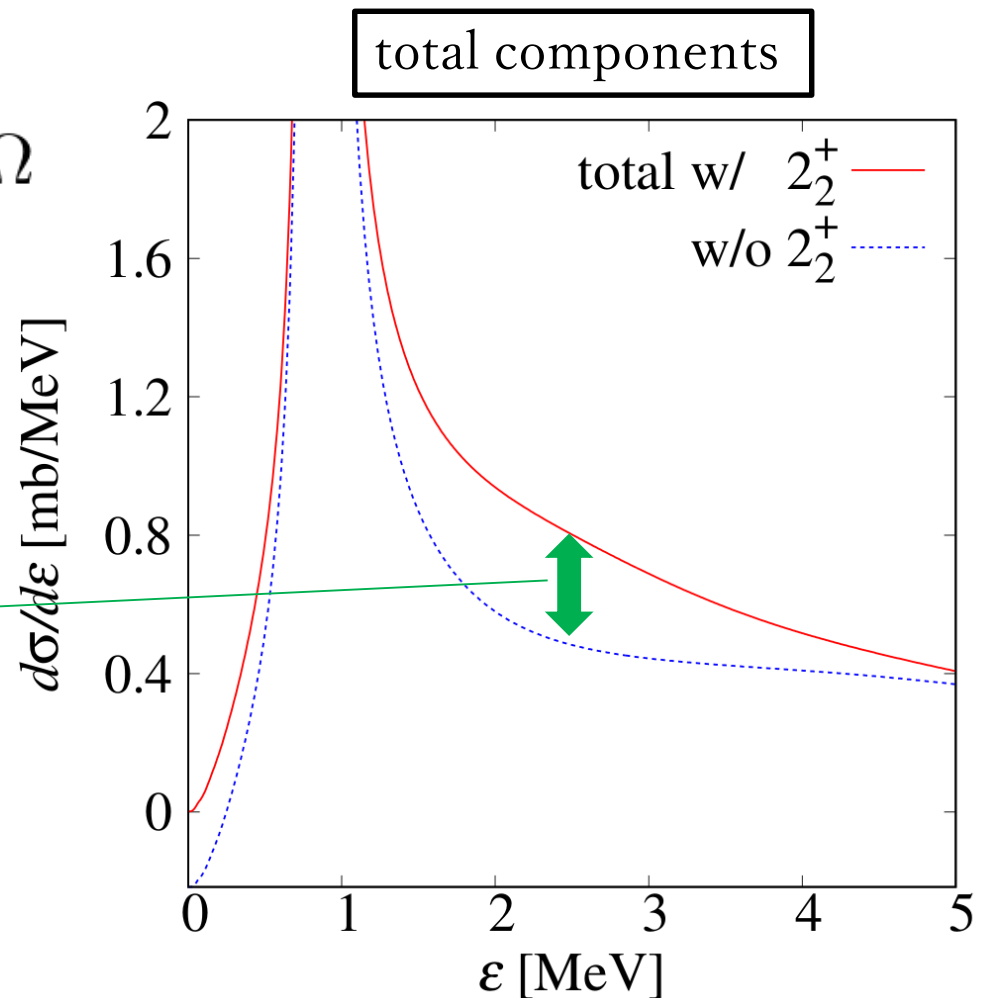
- The shoulder peak comes from 2_2^+ in 2~3 MeV.

Energy spectrum (total)

$$E/A=41\text{MeV}$$

$$\frac{d\sigma}{d\varepsilon} = \int_{20^\circ \leq \theta \leq 30^\circ} \frac{d^2\sigma}{d\varepsilon d\Omega} d\Omega$$

Calc.		
I^π	E	Γ
2_1^+	0.848	0.136
2_2^+	2.25	3.75
0_2^+	3.70	7.13
1_2^-	4.51	8.23
1_1^-	4.42	4.82



- The difference between w/ and w/o 2_2^+ appears in 2~3 MeV.

Summary

We analyze the effects from 2_2^+ on the observables via ${}^6\text{He}(p, p')$ reactions with CDCC and CSM.

CSM

- The result of 2_2^+ is similar to one of previous study which calculated by CSM.

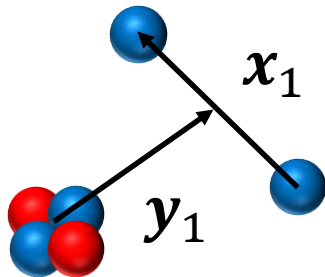
${}^6\text{He}(p, p')$ reactions

- The coupling effects are important.
- In 2^+ component, 2_2^+ appears as like a shoulder peak.

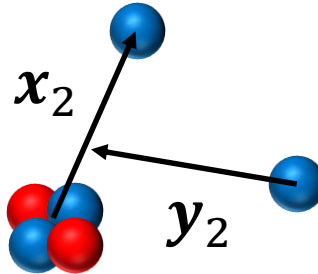
backup

Gaussian Expansion Method

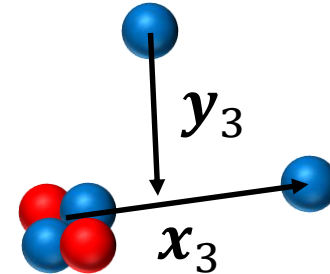
Wavefunctions of ${}^6\text{He}$ are spanned with Gaussian basis functions.



$c = 1$



$c = 2$



$c = 3$

$$\Phi_{Im}(\mathbf{x}, \mathbf{y}) = \sum_{c=1}^3 \sum_{i,j,l,\lambda} \phi_{i,l}(x_c) \varphi_{j,\lambda}(y_c) [[Y_l(\hat{\mathbf{x}}_c) \otimes Y_\lambda(\hat{\mathbf{y}}_c)]_\Lambda \otimes [\eta_{1/2} \otimes \eta_{1/2}]_S]_{Im}$$

$$\phi_{i,l}(x_c) = x_c^l e^{-(x_c/x_i)^2}$$

$$\varphi_{j,\lambda}(y_c) = y_c^\lambda e^{-(y_c/y_j)^2}$$

$$x_i = x_1 \left(\frac{x_{\max}}{x_1} \right)^{\frac{i-1}{i_{\max}-1}}$$

$$y_j = y_1 \left(\frac{y_{\max}}{y_1} \right)^{\frac{j-1}{j_{\max}-1}}$$

✓ n - n interaction : Minnesota D. R. Thompson, *et al.*, Nucl. Phys. A 286 (1977), 53.

✓ n - α interaction : KKNN H. Kanada, *et al.*, Prog. Theor. Phys. 61 (1979), 1327.

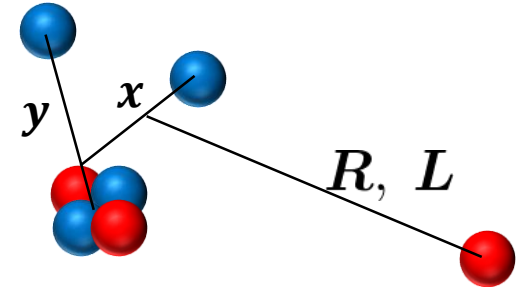
CDCC equation

CDCC wavefunction

$$\Psi_{JM}^{\text{CDCC}}(\xi, \mathbf{R}) = \sum_{I,n} \sum_{L=|J-I|}^{J+I} \frac{\chi_{nIL}(K_n, R)}{R} \mathcal{Y}_{JM}^{nIL}(\xi, \hat{\mathbf{R}})$$

$$K_n = \frac{\sqrt{2\mu(E - \epsilon_n^I)}}{\hbar} \quad \mathcal{Y}_{JM}^{nIL}(\xi, \hat{\mathbf{R}}) = \left[\Phi_n^I(\xi) \otimes i^L Y_L(\hat{\mathbf{R}}) \right]_{JM}$$

$\xi = \{\mathbf{x}, \mathbf{y}\}$ J, M : total spin and its projection on z-axis, I : spin of ${}^6\text{He}$



Schrödinger equation of radial direction

$$\left[-\frac{\hbar^2}{2\mu} \frac{d^2}{dR^2} + \frac{\hbar^2}{2\mu} \frac{L(L+1)}{R^2} + U_{\gamma\gamma} + \frac{Z_p Z_{6\text{He}} e^2}{R} - (E - \epsilon_n^I) \right] \chi_\gamma(K_n, R) = - \sum_{\gamma' \neq \gamma} U_{\gamma\gamma'} \chi_{\gamma'}(K_{n'}, R)$$

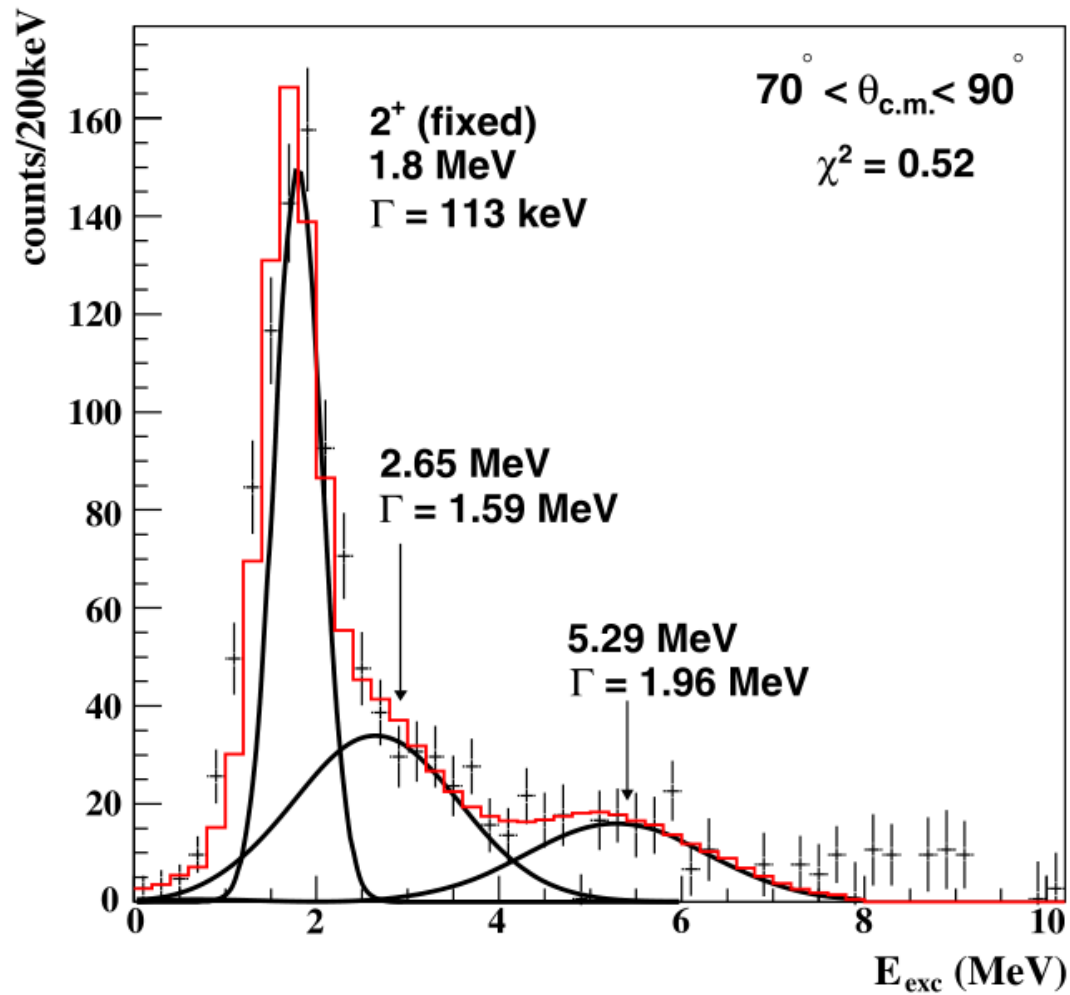
$$U_{\gamma\gamma'}(R) = \frac{A_P - 1}{A_P} \int \rho_{\gamma\gamma'}(\mathbf{s}, \hat{\mathbf{R}}) g_i(E, \bar{\rho}, \mathbf{R}_j) d\mathbf{s} d\hat{\mathbf{R}} \quad \gamma = \{n, I, L\}$$

JLM effective NN interaction

$$\rho_{\gamma\gamma'}(\mathbf{s}, \hat{\mathbf{R}}) = \langle \mathcal{Y}_{JM}^\gamma | \sum_{i \in {}^6\text{He}} \delta(\mathbf{s} - \mathbf{s}_i) | \mathcal{Y}_{JM}^{\gamma'} \rangle_\xi \quad \bar{\rho}(s) = \frac{1}{2} \int \{ \rho_{\gamma\gamma}(\mathbf{s}, \hat{\mathbf{R}}) + \rho_{\gamma'\gamma'}(\mathbf{s}, \hat{\mathbf{R}}) \} d\hat{\mathbf{s}} d\hat{\mathbf{R}}$$

This is calculated with ${}^6\text{He}$ wavefunction.

$$p(^8\text{He}, t)$$



X. Mougeot, et al., Phys. Lett. B 718 (2012), 441.